Polymer Journal (2011) 43, 147–154

www.nature.com/pj

ORIGINAL ARTICLE

Asymmetric anionic polymerization of *N*-substituted maleimides bearing an azo group with chiral anionic initiators

Tsutomu Oishi, Motohisa Azechi, Kanako Kamei, Yukio Isobe and Kenjiro Onimura

Asymmetric anionic homopolymerizations of *N*-substituted maleimides bearing an azo group (RMI: R=4-(phenylazo)phenyl (PAPMI), 4-(phenylazo)-1-naphthyl (PANMI)) were performed with *n*-BuLi or Et_2Zn–chiral ligand ((1-ethylpropylidene)bis (4-benzyl-2-oxazoline) (Bnbox) or (−)-sparteine (Sp)) complexes to obtain optically active polymers. The optical activity of poly(RMI) was influenced by *N*-substituent and polymerization conditions such as organometal type, structure of the chiral ligand, temperature and solvent type. The poly(PANMI) obtained with an *n*-BuLi–Bnbox complex in tetrahydrofuran showed the highest specific rotation ($[\alpha]_D^{25}$=+391.1°). *Trans–cis* photoisomerizations of poly(PAPMI) and poly(PANMI) caused by ultraviolet (UV) irradiation were observed from UV spectra. The rate of *trans–cis* photoisomerization for poly(PAPMI) was faster than that for poly(PANMI). The Cotton effects for *trans* isomers of poly(PAPMI) and poly(PANMI) were relatively small, but those for *cis* isomers of poly(PAPMI) and poly(PANMI) clearly exhibited a split circular dichroism curve.
Polymer Journal (2011) **43,** 147–154; doi:10.1038/pj.2010.126; published online 8 December 2010

Keywords: asymmetric anionic polymerization; azo groups; chiral maleimide

INTRODUCTION

The conformational transformation of polymers is attractive from the standpoint of chiroptical properties, and much research has been conducted on this transformation. In particular, polyacetylene[1–4] and polyisocyanate,[5] with acidic or basic groups in their side chains, exhibit a very interesting property called 'induced helix'. When optically active acids or bases exist in solution with these polymers, the polymers can form one-handed helical conformations by acid–base complexation. This 'induced helix' was confirmed in polyacetylene having an optically active substituent.[4,6] It is notable that the helical sense of these polymers can be controlled by the absolute configuration of the chiral acid and base. In addition, it is also known that optically active polyisocyanates prepared from achiral monomers[7,8] with chiral anionic initiators and optically active monomers[9–11] reveal a temperature-dependent helix–helix inversion.

Some polymers with azo groups in their side chains are interesting because conformational changes in these polymers are induced by the *trans–cis* photoisomerization of azo groups, which are unique chromophores because of their photosensitivity. There have been a number of reports on the conformational switching of optically active polymers bearing azo chromophores. For example, helical polyisocyanate[12–16] with an optically active azo pendant group exhibits a helix inversion triggered by the isomerization of the azo group. Previously, Carlini and coworkers[17,18] reported radical copolymerizations of *N*-(4-phenylazo)-phenylmaleimide (PAPMI) with (+)-menthyl vinyl ether and (−)-menthyl vinyl ether and chiroptical properties of the obtained copolymers. However, there are no reported investigations on homopolymerizations of *N*-substituted maleimide (RMI) bearing an azo chromophore by the asymmetric anionic method.

In this paper, asymmetric anionic polymerizations of two types of RMIs, PAPMI and *N*-(4-phenylazo)-1-naphthylmaleimide (PANMI), were carried out using chiral complexes consisting of organometals and chiral ligands (Scheme 1). The formed polymer was characterized by gel permeation chromatography, D-line-specific rotation ($[\alpha]_D^{25}$) and nuclear magnetic resonance (NMR) spectra. The change in the chiroptical properties of the polymers during *trans*-to-*cis* photoisomerization was investigated by ultraviolet (UV) and circular dichroism (CD) spectra.

EXPERIMENTAL PROCEDURE

Monomer

PAPMI and PANMI were synthesized from maleic anhydride and the corresponding amine according to the reported methods.[19,20]

N-(4-phenylazo)phenylmaleimide

A solution of *para*-aminoazobenzene (1.0 g, 5.0 mmol) in dry benzene (20 ml) was added dropwise to a solution of maleic anhydride (0.5 g, 5.0 mmol) in dry benzene (15 ml) at room temperature over a period of 30 min. Orange precipitates appeared during the reaction. The mixed solution was stirred for an additional 12 h. Precipitates were collected by filtration and washed with

Department of Applied Chemistry, Graduate School of Science and Engineering, Yamaguchi University, Yamaguchi, Japan
Correspondence: Professor T Oishi, Department of Applied Chemistry, Graduate School of Science and Engineering, Yamaguchi University, 2-16-1 Tokiwadai, Ube, Yamaguchi 755-8611, Japan.
E-mail: oishi@yamaguchi-u.ac.jp
Received 3 September 2010; revised 25 October 2010; accepted 26 October 2010; published online 8 December 2010

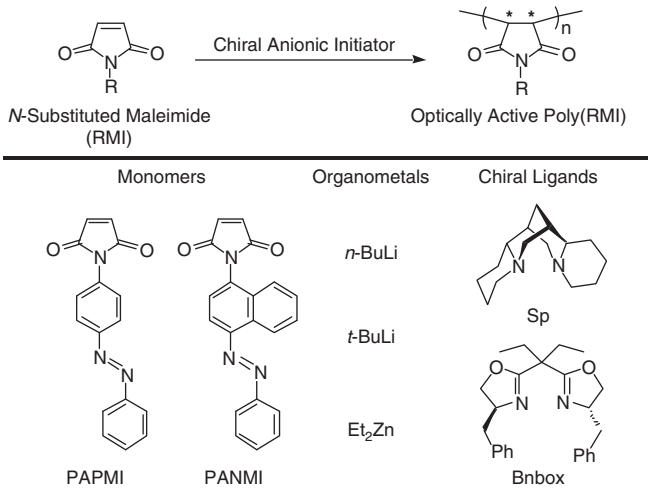

Scheme 1 Polymerizations of RMI.

benzene, water and methanol, in that order. The obtained *N*-(4-phenylazo)-phenylmaleamic acid (PAPMA) was added to toluene (50 ml) and evaporated to dryness to remove residual water by azeotropic distillation. PAPMA was immediately used for the next step without further purification (yield, 1.4 g, 4.7 mmol (94%)). PAPMA (1.4 g, 4.7 mmol) in a dry benzene (100 ml) suspension was heated at 50 °C, after which $ZnBr_2$ (1.1 g, 4.7 mmol) was directly added in one portion. The suspension was refluxed, and 1, 1, 1, 3, 3, 3-hexamethyldisilazane (HMDS, 1.5 ml, 4.7×1.5 mmol) in dry benzene (50 ml) solution was slowly added dropwise to the heated mixture over a period of 30 min, with vigorous stirring. The reaction mixture was refluxed for an additional 4 h. After cooling to room temperature, the reaction mixture was filtered through filter paper, and the filtrate was washed with 0.5 N HCl aq. (50 ml×3), saturated $NaHCO_3$ aq. (50 ml×2) and saturated NaCl aq. (50 ml), in that order. The benzene solution was separated and dried over anhydrous $MgSO_4$. The solution was concentrated to dryness. The crude PAPMI was purified by column chromatography using benzene as an eluent to obtain pure PAPMI as a yellow solid (total yield, 1.2 g (87%); melting point, 160–163 °C; proton NMR (^{1}H NMR; δ in p.p.m. from tetramethylsilane (TMS) in $CDCl_3$): 6.96 (s, 2H, –CH=CH–) and 7.45–8.10 (m, 9H, aromatic protons); carbon-13 NMR (^{13}C NMR; δ in p.p.m. from TMS in $CDCl_3$): 169.16 (carbonyl groups), 134.34 (–C=C– in imide ring), 151.28, 131.27, 129.09, 126.78, 123.50 and 122.95 (phenyl groups)).

N-(4-phenylazo)-1-naphthylmaleimide

PANMI was synthesized following a similar procedure as that used to synthesize PAPMI. Yellow powder (total yield, 91%; melting point, 169–171 °C; ^{1}H NMR (δ in p.p.m. from TMS in $CDCl_3$): 6.96 (s, 2H, –CH=CH–) and 7.45–9.00 (m, 11H, aromatic protons); ^{13}C NMR (δ in p.p.m. from TMS in $CDCl_3$): 169.16 (carbonyl groups), 134.66 (–C=C– in imide ring), 152.52, 151.28, 132.20, 131.68, 131.95, 130.26 and 123.48 (phenyl and naphthyl groups)).

Chiral ligand

Bnbox ((1-ethylpropylidene)bis(4-benzyl-2-oxazoline)) was prepared from (*S*)-phenylalaninol and diethylmalonyl dichloride according to the literature ($[\alpha]_{435}^{25}$=−150.7°, *c*=1.0 g per 100 ml, *l*=10 cm, tetrahydrofuran (THF)).[21,22] (−)-Sparteine (Sp; Ishizu Seiyaku, Osaka, Japan) was distilled immediately before polymerization ($[\alpha]_{435}^{25}$=−10.3°, *c*=1.0 g per 100 ml, *l*=10 cm, THF).

Reagents and solvents

Commercially available organometals, that is, *n*-BuLi and Et_2Zn in an *n*-hexane solution (Kanto Chemical, Tokyo, Japan), were used without purification. Solvents used for syntheses, polymerizations and measurements were purified in the usual manner.

Polymerization

Anionic polymerization was carried out by adding a chiral complex to a monomer solution under a dry nitrogen atmosphere at 0 °C for 72 h. The polymerization was terminated by methanol containing a small amount of HCl aq. The polymer was precipitated from polymerization solvent by dilution with a large amount of methanol. The precipitate was collected by suction filtration and washed with methanol. The polymer was further purified twice by reprecipitation using THF–methanol or $CHCl_3$–trifluoroacetic acid–methanol systems. The purified polymer was dried under vacuum at room temperature for 2 days before characterization.

Spectroscopic data of poly(PAPMI): Infrared (IR) (KBr) 1386 cm^{-1} ($\nu_{N=N}$) and 1705 cm^{-1} ($\nu_{C=O}$); ^{1}H NMR ($CDCl_3$) δ 2.9–4.8 p.p.m. (br, –CH–CH–, 2H) and 6.0–8.2 p.p.m. (br, aromatic, 9H). ^{13}C NMR ($CDCl_3$) δ 40.0–50.0 p.p.m. (br, –CH–CH–), 120.8, 123.1, 127.4, 129.0, 131.1, 149.2 and 151.9 p.p.m. (br, aromatic) and 176.3 p.p.m. (br, C=O).

Spectroscopic data of poly(PANMI): IR (KBr) 1363 cm^{-1} ($\nu_{N=N}$) and 1704 cm^{-1} ($\nu_{C=O}$); ^{1}H NMR ($CDCl_3$) δ 3.5–4.6 p.p.m. (br, –CH–CH–, 2H) and 6.0–9.1 p.p.m. (br, aromatic, 11H). ^{13}C NMR ($CDCl_3$) δ 39.0–49.0 p.p.m. (br, –CH–CH–), 110.0, 123.3, 126.8, 129.9, 130.7, 148.4 and 152.9 p.p.m. (br, aromatic) and 176.3 p.p.m. (br, C=O).

Measurements

Hg- ($[\alpha]_{435}^{25}$) and D-line ($[\alpha]_{D}^{25}$)-specific rotations were measured at 25 °C in THF or $CHCl_3$–trifluoroacetic acid (9/1 (v/v)) using a JASCO DIP-140 (JASCO, Tokyo, Japan). ^{1}H- (270 MHz) and ^{13}C NMR (68 MHz) spectra were obtained using a JEOL EX-270 (JEOL, Tokyo, Japan) and TMS as an internal standard. Gel permeation chromatography was performed using a Shimadzu chromatopac C-R7Ae plus (Shimadzu, Kyoto, Japan) equipped with a Shimadzu SPD-10A UV detector (254 nm; Shimadzu) and a JASCO-OR 990 polarimetric detector (350–900 nm) (JASCO); THF was used as an eluent at 50 °C to calculate the number-average molecular weight ($\bar{M}_n$) and molecular weight distribution ($\bar{M}_w/\bar{M}_n$) with polystyrene as a standard. UV and CD spectra were obtained in a quartz cell at 25 °C with a Shimadzu UV-2200 (Shimadzu) and a JASCO J-20C apparatus (JASCO), respectively.

RESULTS AND DISCUSSION

Polymerizations of PAPMI

The conditions and results of the polymerizations of PAPMI with *n*-BuLi and alkyllithium–chiral ligand complexes are summarized in Table 1. Anionic polymerization of PAPMI without a chiral ligand produced the methanol-insoluble polymer in a 12% yield (run 1 in Table 1). However, the conversion was 100%, and the monomer did not exist in the reaction solution after polymerization, as observed on the basis of NMR spectra; that is, the methanol-insoluble part of the polymer was very low in yield and had an $\bar{M}_n$ of 1300. The methanol-soluble part of the polymer was ∼88% of the yield and had an $\bar{M}_n$ <800. Using an organometal–chiral ligand complex as an initiator, the polymer yields improved, as shown in Table 1. A similar tendency was observed in the polymerizations of RMI in many of our previous papers.[23,24] As a whole, the number-average molecular weights of the formed polymers were low ($\bar{M}_n$=900–4200), suggesting that the bulkiness of the *N*-substituent inhibits the polymerizability. All polymerizations using chiral ligand complexes produced optically active polymers. The specific rotations of the poly(PAPMI)s prepared with the alkyllithium–chiral ligand in toluene (runs 3, 5, 7 and 9 in Table 1) exhibited a sign opposite of that prepared with the same initiator in THF (runs 4, 6, 8 and 10). In addition, the sign of the specific rotations of the poly(PAPMI)s obtained with the *n*-BuLi–chiral ligand in toluene or THF was opposite to that obtained with the *t*-BuLi–chiral ligand in the same solvent. These results indicate that the sign of the optical activity depends not only on the chiral ligand but also on the solvent and the alkyl group bonded to lithium metal. The absolute

Table 1 Anionic polymerizations of PAPMI with alkyllithium–chiral ligand complex

Run	PAPMI (mol/l)[a]	Initiator[b]	Polymerization solvent (ml)	Polymerization temperature (°C)	Polymerization time (h)	Yield[c] (%)	$\bar{M}_n \times 10^{-3}$[d]	$\bar{M}_n/\bar{M}_n$[d]	$[\alpha]_D^{25}$ (deg.)[e]
1	0.03	*n*-BuLi	Tol. (22)	0	72	12	1.3	1.2	—
2	0.10	*n*-BuLi	THF (6)	0	72	58	2.2	1.8	—
3	0.02	*n*-BuLi–Sp	Tol. (25)	0	72	69	1.2	1.8	–69.7
4	0.12	*n*-BuLi–Sp	THF (15)	0	72	92	2.8	2.0	+7.8
5	0.02	*t*-BuLi–Sp	Tol. (25)	0	72	48	1.1	1.7	+13.5
6	0.12	*t*-BuLi–Sp	THF (15)	0	72	74	1.7	2.1	–86.4
7	0.02	*n*-BuLi–Bnbox	Tol. (25)	0	72	53	1.1	1.5	–86.5
8	0.12	*n*-BuLi–Bnbox	THF (15)	0	72	76	4.2	3.7	+6.8
9	0.02	*t*-BuLi–Bnbox	Tol. (25)	0	72	52	1.3	1.5	+17.4
10	0.12	*t*-BuLi–Bnbox	THF (15)	0	72	62	0.9	2.4	–4.4

Abbreviations: Bnbox, (1-ethylpropylidene)bis(4-benzyl-2-oxazoline); GPC, gel permeation chromatography; PAPMI, R=4-(phenylazo)phenyl; Sp, (−)-sparteine; THF, tetrahydrofuran; Tol., toluene.
[a]PAPMI: 0.2 g (runs 1, 2, 3, 5, 7 and 9) and 0.5 g (runs 4, 6, 8 and 10).
[b][Alkyllithium]/[PAPMI]=0.1; [alkyllithium]/[chiral ligand]=1.0/1.2.
[c]Methanol—insoluble part.
[d]By GPC using THF as an eluent at 50 °C.
[e]*c*=0.2 g per 100 ml and *l*=10 cm, in THF.

Table 2 Anionic polymerizations of PAPMI with diethylzinc–chiral ligand complex

Run	PAPMI (mol l−1)[a]	Initiator ([organometal]/[ligand])[b]		Polymerization solvent (ml)	Polymerization temperature (°C)	Polymerization time (h)	Yield (%)[c]	$\bar{M}_n \times 10^{-3}$[d]	$\bar{M}_n/\bar{M}_n$[d]	$[\alpha]_D^{25}$ (deg.)[e]
1	0.02	Et_2Zn–Sp	(1.0/1.2)	Tol. (25)	0	72	23	3.0	1.6	+8.6
2	0.12	Et_2Zn–Sp	(1.0/1.2)	THF (15)	0	72	69	3.9	1.6	+24.4
3	0.02	Et_2Zn–Bnbox	(1.0/1.2)	Tol. (25)	0	72	23	1.9	1.2	+41.7
4	0.12	Et_2Zn–Bnbox	(1.0/1.2)	THF (15)	0	72	25	7.0	2.3	–124.1
5	0.04	Et_2Zn–Bnbox	(1.0/0.5)	Tol. (50)	0	72	73	(4.0)[g]	(1.6)[g]	–279.8[f] (–74.9)[g,h]
6	0.12	Et_2Zn–Bnbox	(1.0/0.5)	THF (15)	0	72	100	(5.6)[g]	(1.8)[g]	–313.3[f] (–90.7)[g,h]
7	0.05	Et_2Zn–Bnbox	(1.0/0.5)	THF (15)	0	72	64	4.2	1.6	–177.6[f] (–78.6)[g,h]

Abbreviations: Bnbox, (1-ethylpropylidene)bis(4-benzyl-2-oxazoline); GPC, gel permeation chromatography; PAPMI, R=4-(phenylazo)phenyl; Sp, (−)-sparteine; THF, tetrahydrofuran; Tol., toluene.
[a]PAPMI: 0.2 g (runs 1, 3, 5 and 7) and 0.5 g (runs 2, 4 and 6).
[b][Diethylzinc]/[PAPMI]=0.1.
[c]Methanol—insoluble part.
[d]By GPC using THF as an eluent at 50 °C.
[e]*c*=0.2 g per 100 ml and *l*=10 cm, in THF.
[f]Poly(PAPMI) obtained was not completely dissolved in THF. *c*=0.2 g per 100 ml and *l*=5 cm, in $CHCl_3$/trifluoroacetic acid=9.5/0.5 (v/v).
[g]Data in parenthesis is due to THF-soluble parts in poly(PAPMI).
[h]*c*=0.2 g per 100 ml and *l*=10 cm, in THF.

value of the specific rotation of the poly(PAPMI) formed in toluene was higher than that formed in THF, except for *t*-BuLi–Sp systems, suggesting that the use of a polar solvent such as THF disturbs the asymmetric synthesis with *n*-BuLi–Sp, *n*-BuLi–Bnbox and *t*-BuLi–Bnbox complexes.

Table 2 lists the conditions and results of the polymerizations of PAPMI using Et_2Zn–chiral ligand complexes. Compared with the results of Table 1, high-molecular-weight poly(PAPMI) was obtained by using Et_2Zn–chiral ligand complexes ($\bar{M}_n$=1900–7000). All polymers prepared under the conditions listed in Table 2 exhibited optical activity. The poly(PAPMI)s formed with Sp as a chiral ligand in toluene and THF showed dextrorotations ($[\alpha]_D^{25}$=+8.6 and +24.4°). In contrast, poly(PAPMI)s obtained with Bnbox were levorotatory ($[\alpha]_D^{25}$=−313.3 to −124.1°), except for run 3 ($[\alpha]_D^{25}$=+41.7°), and the absolute values were much greater than those of the poly(PAPMI)s initiated with Et_2Zn–Sp and alkyllithium–chiral ligand complexes. Et_2Zn–Bnbox, in particular, is a suitable chiral anionic initiator for the asymmetric polymerization of PAPMI. In all runs, the specific rotations of poly(PAPMI) obtained in THF were higher than those obtained in toluene, suggesting that the optimum symmetric reaction field was built by THF in addition to the chiral ligand at the growing chain end.[23,24] When PAPMI was polymerized with Et_2Zn–Bnbox in THF, the obtained polymers contained THF-insoluble parts (runs 5–7 in Table 2). The polymers were completely dissolved in a mixed solvent of $CHCl_3$ and a small amount of trifluoroacetic acid. In runs 5–7, the specific rotations of the methanol-insoluble polymers containing THF-insoluble parts were much higher than those of the THF-soluble parts; that is, the THF-insoluble parts of poly(PAPMI) showed higher optical activity and poor solubility. This probably indicates that THF-insoluble polymers have crystallinity, which is given by high stereoregularity, that is, optically active *threo*-diisotactic sequences. The molar ratio of [Et_2Zn]/[Bnbox] affected the specific rotation of the poly(PAPMI). The specific rotations of poly(PAPMI)s initiated with the molar ratio of [Et_2Zn]/[Bnbox]=1.0/0.5 were higher than those initiated with the molar ratio of [Et_2Zn]/[Bnbox]=1.0/1.2. This suggests that a better structure of the initiator complex is formed by the ratio of 1.0/0.5; that is, the chiral complex consists of two Et_2Zn and one Bnbox molecule.

Polymerizations of PANMI

Table 3 summarizes the polymerization results of PANMI with alkyllithium–chiral ligand complexes. The yields and number-average

Table 3 Anionic polymerizations of PANMI with alkyllithium–chiral ligand complex

Run	PANMI (mol/l)[a]	Initiator[b]	Polymerization solvent (ml)	Polymerization temperature (°C)	Polymerization time (h)	Yield (%)[c]	$\bar{M}_n \times 10^{-3}$[d]	$\bar{M}_w/\bar{M}_n$[d]	$[\alpha]_D^{25}$ (deg.)[e]
1	0.09	*n*-BuLi	Tol. (7)	0	72	23	1.7	1.6	—
2	0.15	*n*-BuLi	THF (4)	0	72	66	2.8	2.2	—
3	0.05	*n*-BuLi–Sp	Tol. (16)	0	72	69	1.3	2.6	−81.7
4	0.15	*n*-BuLi–Sp	THF (10)	0	72	100	2.8	2.6	+71.1
5	0.05	*t*-BuLi–Sp	Tol. (16)	0	72	82	2.1	1.6	−7.0
6	0.15	*t*-BuLi–Sp	THF (10)	0	72	100	3.6	2.6	−108.7
7	0.05	*n*-BuLi–Bnbox	Tol. (16)	0	72	74	2.5	1.7	−186.8
8	0.15	*n*-BuLi–Bnbox	THF (10)	0	72	100	3.8	1.6	+391.1
9	0.05	*t*-BuLi–Bnbox	Tol. (16)	0	72	96	1.8	1.8	+11.0
10	0.15	*t*-BuLi–Bnbox	THF (10)	0	72	96	1.1	2.2	−3.3

Abbreviations: Bnbox, (1-ethylpropylidene)bis(4-benzyl-2-oxazoline); GPC, gel permeation chromatography; PANMI, 4-(phenylazo)-1-naphthyl; Sp, (−)-sparteine; THF, tetrahydrofuran; Tol., toluene.
[a]PANMI: 0.2 g (runs 1, 2, 3, 5, 7 and 9) and 0.5 g (runs 4, 6, 8 and 10).
[b][Organometal]/[PANMI]=0.1; [alkyllithium]/[chiral ligand]=1.0/1.2.
[c]Methanol—insoluble part.
[d]By GPC using THF as an eluent at 50 °C.
[e]*c*=0.2 g per 100 ml and *l*=10 cm, in THF.

Table 4 Anionic polymerizations of PANMI with diethylzinc–chiral ligand complex

Run	PANMI (mol/l)[a]	Initiator ([organometal]/[ligand])[b]		Polymerization solvent (ml)	Polymerization temperature (°C)	Polymerization time (h)	Yield (%)[c]	$\bar{M}_n \times 10^{-3}$[d]	$\bar{M}_w/\bar{M}_n$[d]	$[\alpha]_D^{25}$ (deg.)[e]
1	0.05	Et_2Zn–Sp	(1.0/1.2)	Tol. (16)	0	72	69	2.6	2.0	+65.6
2	0.15	Et_2Zn–Sp	(1.0/1.2)	THF (10)	0	72	36	2.4	1.5	+19.2
3	0.05	Et_2Zn–Bnbox	(1.0/1.2)	Tol. (16)	0	72	50	2.8	1.9	−139.9
4	0.15	Et_2Zn–Bnbox	(1.0/1.2)	THF (10)	0	72	21	2.4	1.4	−38.8
5	0.04	Et_2Zn–Bnbox	(1.0/0.5)	Tol. (40)	0	72	89	4.0	1.6	−156.3
6	0.15	Et_2Zn–Bnbox	(1.0/0.5)	THF (10)	0	72	100	5.6	1.8	−190.7

Abbreviations: Bnbox, (1-ethylpropylidene)bis(4-benzyl-2-oxazoline); GPC, gel permeation chromatography; PANMI, 4-(phenylazo)-1-naphthyl; Sp, (−)-sparteine; THF, tetrahydrofuran; Tol., toluene.
[a]PANMI: 0.2 g (runs 1 and 3) and 0.5 g (runs 2, 4, 5 and 6).
[b][Organometal]/[PANMI]=0.1.
[c]Methanol—insoluble part.
[d]By GPC using THF as an eluent at 50 °C.
[e]*c*=0.2 g per 100 ml (runs 1–4), *c*=1.0 g per 100 ml (runs 5 and 6) and *l*=10 cm, in THF.

molecular weights were higher than those listed in Table 1 because PANMI has higher solubility than PAPMI. In all polymerizations using chiral ligands, the obtained poly(PANMI) exhibited optical activity. The use of *n*-BuLi–Bnbox as an initiator produced highly optically active poly(PANMI)s ($[\alpha]_D^{25}$=−186.8 and +391.1°). However, the poly(PANMI)s obtained with *t*-BuLi–Bnbox (runs 9 and 10 in Table 3) exhibited very low specific rotations ($[\alpha]_D^{25}$=+11.0 and −3.3°), despite possessing the same chiral ligand as in runs 7 and 8. This may result from the fact that the $\bar{M}_n$ of the polymers obtained with *t*-BuLi were 1000 to 1800, as shown in Table 3, which are relatively lower than those obtained with *n*-BuLi. The specific rotations of the poly(PANMI)s initiated with alkyllithium–Bnbox in toluene showed an opposite sign to those of the poly(PANMI)s obtained with the same initiator in THF. On the basis of these results, it was found that alkyl groups that coordinated to lithium, as well as to Bnbox, could influence the asymmetric synthesis during polymerization.

The polymerization conditions and results of PANMI using Et_2Zn–chiral ligand complexes are listed in Table 4. Polymerizations using Sp as a chiral ligand produced levorotatory polymers. In contrast, poly(PANMI)s prepared using Bnbox exhibited dextrorotations. These results are similar to those of the polymerization of PAPMI (see runs 3–7 in Table 2). That is, when Et_2Zn is used as the initiator complex, asymmetric synthesis is controlled only by the chirality of the chiral ligand. In the polymerization using Et_2Zn–Bnbox, the specific rotations of the poly(PANMI)s formed with the molar ratio of [Et_2Zn]/[Bnbox]=1.0/0.5 ($[\alpha]_D^{25}$=−156.3 and −190.7°) were higher than those formed with the ratio of 1.0/1.2 ($[\alpha]_D^{25}$=−139.9 and −38.8°). Furthermore, there is a significant gap in the specific rotations between poly(PAPMI)s (runs 4 and 6 in Table 4) formed by the different ratios in THF, indicating that the molar ratio significantly influences the asymmetric polymerization of PANMI in THF.

Chiroptical properties of polymers

To investigate the optical rotation of every molecular weight part in the polymers, gel permeation chromatography chromatograms were recorded by UV and polarimetric (α_{Hg}) detectors. The obtained chromatograms are displayed in Figure 1. Chromatograms (A) and (B) in Figure 1 are due to the poly(PAPMI)s obtained with *n*-BuLi–Sp (run 4 in Table 1, $[\alpha]_D^{25}$=+7.8°) in THF and Et_2Zn–Bnbox in THF (run 4 in Table 2, $[\alpha]_D^{25}$=−124.1°), respectively. Chromatograms (C) and (D) are due to the poly(PANMI)s formed with *t*-BuLi–Sp in THF (run 6 in Table 3, $[\alpha]_D^{25}$=−108.7°) and Et_2Zn–Bnbox in THF (run 6 in Table 4, $[\alpha]_D^{25}$=−190.7°), respectively. In each polymer, the α_{Hg} curve corresponds to a UV curve. Moreover, the top of the α_{Hg} curve is in fair agreement with that of the UV curve. From these results, it is clear that every molecular weight part in each polymer possesses the same

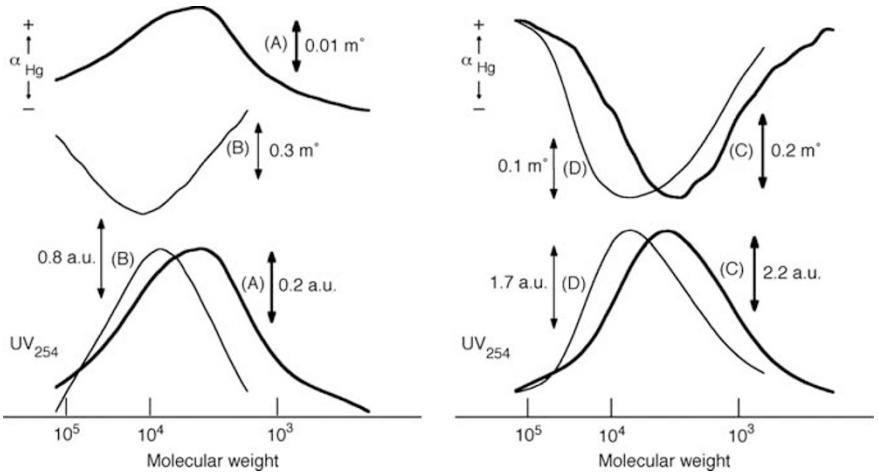

Figure 1 Gel permeation chromatography curves of poly(PAPMI) ((A), run 4 in Table 1; $[\alpha]_D$=+7.8°; (B), run 4 in Table 2; $[\alpha]_D$=–124.1°) and poly(PANMI) ((C), run 6 in Table 3; $[\alpha]_D$=–108.7°; (D), run 6 in Table 4; $[\alpha]_D$=–190.7°). The top chromatograms were measured by a polarimetric detector (α_{Hg}) and the bottom ones by an ultraviolet (UV) detector (254 nm). PANMI, R=4-(phenylazo)-1-naphthyl; PAPMI, R=4-(phenylazo) phenyl.

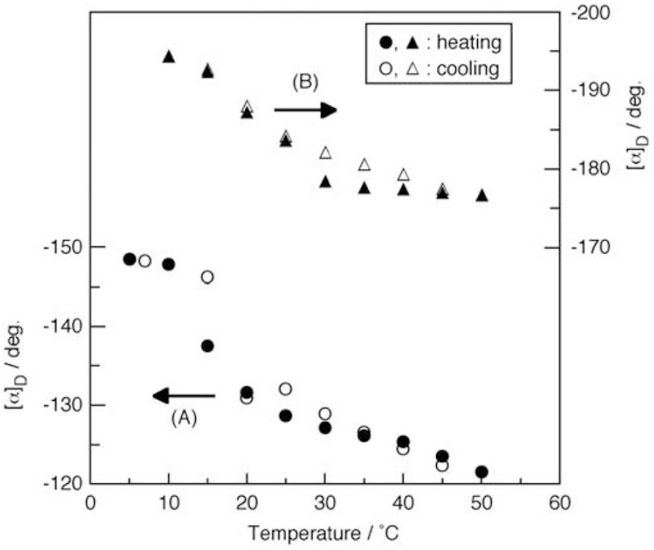

Figure 2 Change in the specific rotation of poly(PAPMI) ((A), run 4 in Table 2) and poly(PANMI) ((B), run 6 in Table 4) with temperature. PANMI, R=4-(phenylazo)-1-naphthyl; PAPMI, R=4-(phenylazo) phenyl.

optical rotation; that is, the optical activity of the polymers is independent of the molecular weight. This also means that similar asymmetric addition reactions constantly take place during the polymerization.

Highly optically active poly(PAPMI) and poly(PANMI) may contain chiral conformations, such as partial helical sequences induced by high continuity of *threo*-diisotactic units. To investigate this point further, the specific rotations of these polymers were measured at several temperatures. Figure 2 depicts the changes in the specific rotations of poly(PAPMI) ((A), run 4 in Table 2, $[\alpha]_D^{25}=-124.1°$) and poly(PANMI) ((B), run 6 in Table 4, $[\alpha]_D^{25}=-190.7°$) with temperature. The specific rotations of these polymers decreased with heating and increased with cooling. The gaps between the maximum and minimum specific rotations of poly(PAPMI) and poly(PANMI) were 27.0 and 17.7°, respectively, and these changes were reversible. In Figure 2, the specific rotation of poly(PAPMI) showed a discontinuous change between 10 and 20 °C (A). On the other hand, as shown by (B), the degree to which the specific rotation of poly(PANMI) changed between 10 and 30 °C was different from that between 30 and 50 °C. These changes are probably attributable to the relaxation of chiral conformations such as helical sequences given by continuous (*S*, *S*)- or (*R*, *R*)-*threo*-diisotactic main chains. In addition, the discontinuity in Figure 2 indicates that the chiral conformations of the polymers change dramatically in those temperature regions.

Photoisomerizations of polymers

To analyze the photoisomerizations of the azo groups in PAPMI and poly(PAPMI), UV spectra were measured before and after UV irradiation. Figure 3 shows UV curves (panels a–c) for PAPMI, the THF-soluble part of poly(PAPMI) formed with Et_2Zn–Bnbox in THF (run 7 in Table 2; $[\alpha]_D^{25}=-78.6°$) and poly(PAPMI) formed with Et_2Zn–Bnbox in THF (run 4 in Table 2; $[\alpha]_D^{25}=-124.1°$), respectively. The peak centered at 330 nm in each spectrum is ascribed to the π–π* transition of the *trans*-azo aryl group. The absorbance at 330 nm in the UV spectra decreased with increasing irradiation time. Absorbance due to the π–π* transition of the *trans*-azo aryl group of PAPMI and poly(PAPMI) almost disappeared after 40 min, and remained unchanged afterward, indicating that the *trans*-to-*cis* photoisomerization was complete at 40 min. The rate of *trans*-to-*cis* photoisomerization was the same among PAPMI and poly(PAPMI)s with low- and high specific rotation. This indicates that the photoisomerization rate is not affected by molecular weight and optical activity.

Figure 4 presents the photoisomerization results for PANMI and poly(PANMI). UV curves (panels a–c) are due to PANMI, poly (PANMI) obtained with Et_2Zn–Bnbox in THF (run 6 in Table 4, $[\alpha]_D^{25}=-190.7°$) and poly(PANMI) obtained with *n*-BuLi–Bnbox in THF (run 8 in Table 3, $[\alpha]_D^{25}=+391.1°$), respectively. The peak centered at 380 nm is due to the π–π* transition of the *trans*-azo aryl group, and its intensity decreased with UV irradiation time, indicating that the *trans*-azo forms were transformed into *cis*-azo ones by photoisomerization. The photoisomerizations for PANMI monomer and poly(PANMI) were terminated at 120 and 180 min, respectively. The rate of *trans*-to-*cis* photoisomerization for PANMI monomer was evidently faster than that for its polymers. It can be presumed that an environment that is more crowded for the polymer than for the PANMI monomer prevents the *trans*-to-*cis* photoisomerization. The photoisomerization rate was different among poly

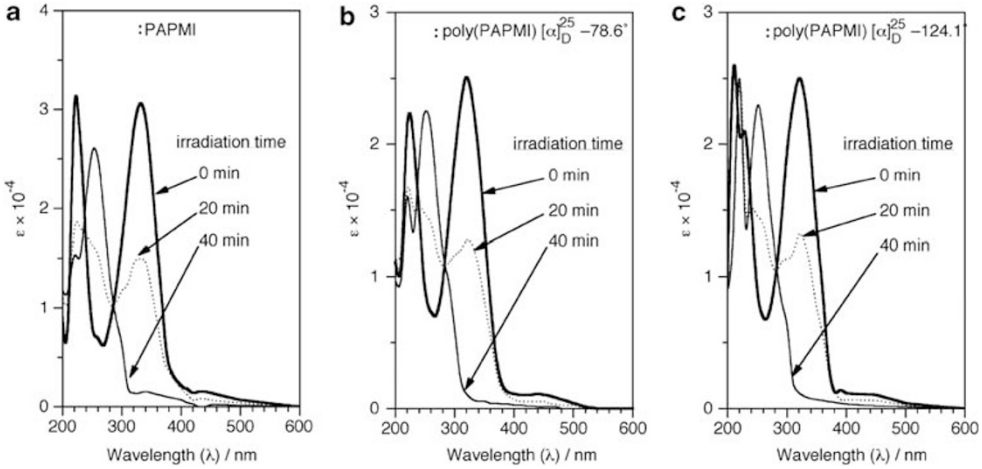

Figure 3 Change in the ultraviolet spectra of PAPMI (**a**) and poly(PAPMI) (**b**, run 7 in Table 2; **c**, run 4 in Table 2) with *trans–cis* photoisomerization of the azo group. PAPMI, R=4-(phenylazo) phenyl.

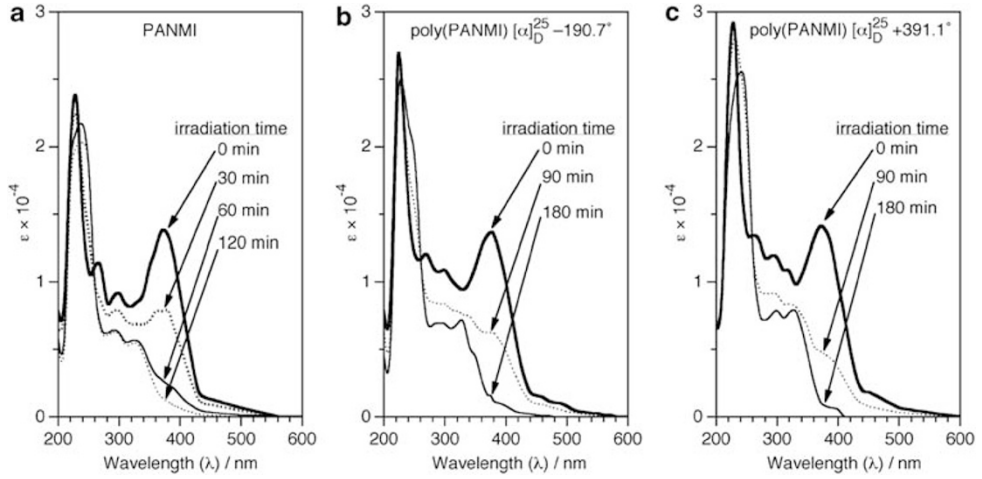

Figure 4 Change in ultraviolet spectra of PANMI (**a**) and poly(PANMI) (**b**, run 6 in Table 4; **c**, run 8 in Table 3) with *trans–cis* photoisomerization of the azo group. PANMI, R=4-(phenylazo)-1-naphthyl.

(PANMI)s. The photoisomerization rate for poly(PANMI) with a higher specific rotation (Figure 4c; $[\alpha]_D^{25}=+391.1^\circ$) was slightly faster than that for poly(PANMI) with a lower specific rotation (Figure 4b; $[\alpha]_D^{25}=-190.7^\circ$). The differences in stereoregularity and/or conformation between the two poly(PANMI)s probably influence the rate of photoisomerization. Compared with the results of the PAPMI series (Figure 3), the photoisomerization rates for the PANMI systems (Figure 4) were very slow. This difference may result from bulkiness of the naphthyl groups bonded to the azo chromophores.

To obtain information about the change in optical activity due to photoisomerization, CD and UV spectra were measured in THF. Figures 5a and b show spectra of poly(PAPMI) prepared with Et_2Zn–Bnbox in THF (run 4 in Table 2; $[\alpha]_D^{25}=-124.1^\circ$) and poly(PANMI) prepared with Et_2Zn–Bnbox in toluene (run 3 in Table 4; $[\alpha]_D^{25}=-139.9^\circ$), respectively. Before photoisomerization, poly(PAPMI) with *trans*-azo chromophores exhibited only a few CD peaks at ~330 nm. However, after photoisomerization, poly(PAPMI) with *cis*-azo chromophores showed obvious split CD patterns. The change in CD spectra was reversible. Poly(PANMI) bearing *trans*-azo groups exhibited a weak and positive CD peak around the UV absorption band, but it changed into split CD patterns with higher molar ellipticity after photoisomerization. The change in CD spectra was also reversible. The azo chromophores are apart from the chiral main chain; nevertheless, they exhibited a distinct CD band after photoisomerization. It seems that the *cis*-azo groups in the polymers can form chiral conformations. In other words, chiral conformations such as helical conformations are induced by *trans*-to-*cis* photoisomerization. There are few data to clearly prove this point, but, as shown in Scheme 2, it can be explained on the basis of steric factors. Steric repulsion due to the *cis*-azo aryl groups among vicinal monomeric units is higher than that due to the *trans*-azo groups so that *N*-pendant groups with *cis*-azo groups are as apart from each other as possible. Consequently, the polymer backbone with rich *threo*-diisotactic sequences can form more helical conformations than the polymer having *trans*-azo aryl groups.

CONCLUSIONS

Asymmetric anionic polymerizations of achiral RMI-bearing azo groups, PAPMI and PANMI, were achieved with organometal–chiral ligand complexes to obtain optically active polymers. The optical

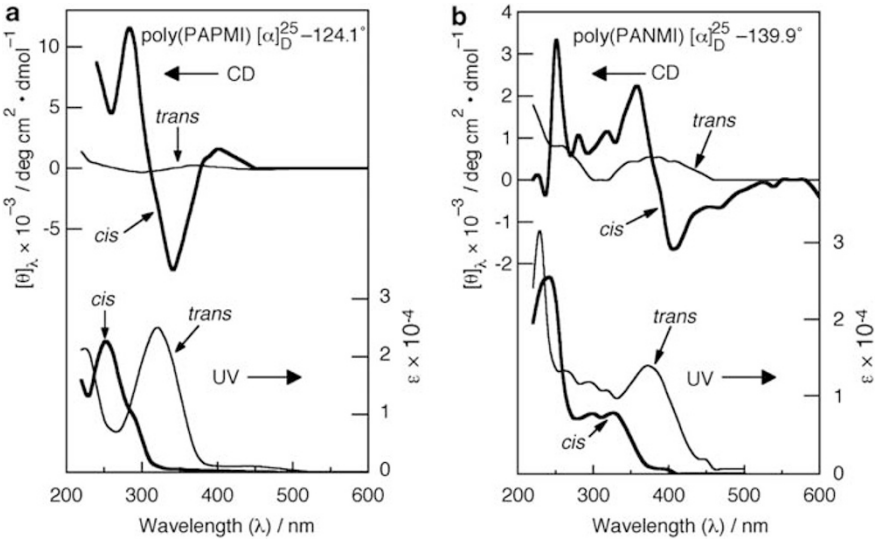

Figure 5 Circular dichroism (CD) and ultraviolet (UV) spectra of poly(PAPMI) (**a**, run 4 in Table 2; $[\alpha]_D = -124.1°$) and poly(PANMI) (**b**, run 3 in Table 4; $[\alpha]_D = -139.9°$) before and after *trans–cis* photoisomerization in tetrahydrofuran. PANMI, R=4-(phenylazo)-1-naphthyl; PAPMI, R=4-(phenylazo) phenyl.

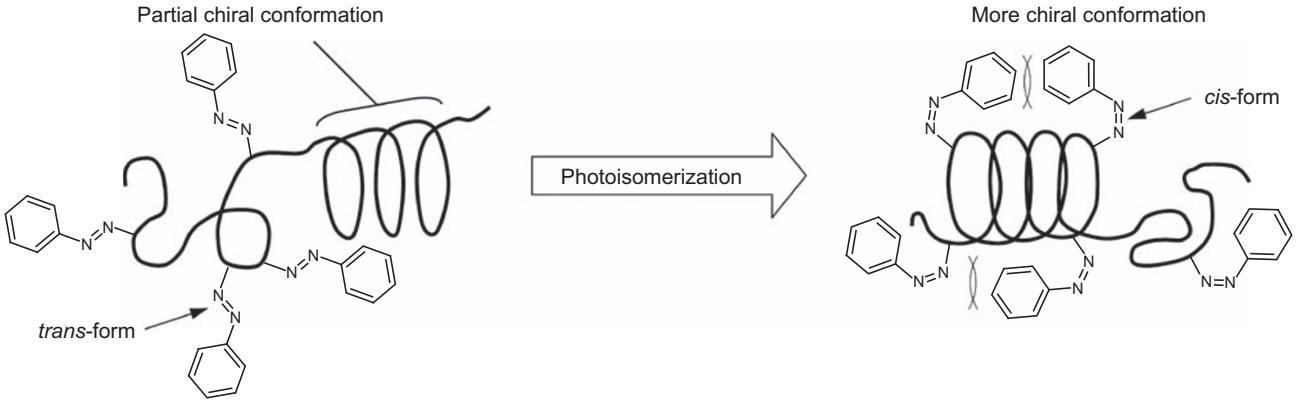

Scheme 2 Photoisomerization of poly(RMI).

activity of poly(RMI) was greatly influenced by the *N*-substituent and polymerization conditions. The poly(PAPMI) prepared with Et_2Zn–Bnbox showed a levo-specific rotation of −313.3°. The poly(PANMI) obtained with *n*-BuLi–Bnbox in THF showed the highest specific rotation of +391.1°. *Trans–cis* photoisomerizations of the polymers caused by UV irradiation were observed by UV spectra. The intensity of the absorption band of the *trans*-azo groups decreased progressively with UV irradiation time. The rate of *trans–cis* photoisomerization for poly(PAPMI) was faster than that for poly(PANMI). There was no difference in the rate of photoisomerization between polymers having different specific rotations. The rate of photoisomerization for poly (PANMI) was faster than that for PANMI. The difference in the rate of photoisomerization between the monomer and polymer could be attributed to steric repulsion by polymeric effects. The Cotton effects for *trans* isomers of poly(PAPMI) and poly(PANMI) were relatively small, but those for *cis* isomers of poly(PAPMI) and poly(PANMI) clearly exhibited a split CD curve, suggesting that the polymers with *cis*-azo groups can form chiral conformations.

1 Yashima, E., Matsushima, T. & Okamoto, Y. Chirality assignment of amines and amino alcohols based on circular dichroism induced by helix formation of a stereoregular poly((4-carboxyphenyl)acetylene) through acid-base complexation. *J. Am. Chem. Soc.* **119,** 6345–6359 (1997).
2 Yashima, E., Goto, H. & Okamoto, Y. Induced helix of an aliphatic polyacetylene detected by circular dichroism. *Polym. J.* **30,** 69–71 (1998).
3 Yashima, E., Maeda, K. & Okamoto, Y. Memory of macromolecular helicity assisted by interaction with achiral small molecules. *Nature* **399,** 449–451 (1999).
4 Yashima, E., Maeda, K. & Okamoto, Y. Synthesis of poly[*N*-(4-ethynylbenzyl)ephedrine] and its use as a polymeric catalyst for enantioselective addition of dialkylzincs to benzaldehyde. *Polym. J.* **31,** 1033–1036 (1999).
5 Maeda, K., Yamamoto, N. & Okamoto, Y. Helicity induction of poly(3-carboxyphenyl isocyanate) by chiral acid-base interaction. *Macromolecules* **31,** 5924–5926 (1998).
6 Yashima, E., Maeda, K. & Okamoto, Y. Helix-helix transition of optically active poly((1R,2S)-N-(4-ethynylbenzyl)norephedrine) induced by diastereomeric acid-base complexation using chiral stimuli. *J. Am. Chem. Soc.* **120,** 8895–8896 (1998).
7 Okamoto, Y., Matsuda, M., Nakano, T. & Yashima, E. Asymmetric polymerization of aromatic isocyanates with optically active anionic initiators. *J. Polym. Sci. A Polym. Chem.* **32,** 309–315 (1994).
8 Maeda, K. & Okamoto, Y. Helical structure of oligo- and poly(m-substituted phenyl isocyanate)s bearing an optically active end-group. *Polym. J.* **30,** 100–105 (1998).
9 Maeda, K. & Okamoto, Y. Synthesis and conformation of optically active poly(phenyl isocyanate)s bearing an ((S)-(α-methylbenzyl)carbamoyl) group. *Macromolecules* **31,** 1046–1052 (1998).
10 Maeda, K. & Okamoto, Y. Unusual conformational change of optically active poly(3-((S)-sec-butoxycarbonyl)phenyl isocyanate). *Macromolecules* **31,** 5164–5166 (1998).
11 Maeda, K. & Okamoto, Y. Synthesis and conformational characteristics of poly (phenyl isocyanate)s bearing an optically active ester group. *Macromolecules* **32,** 974–980 (1999).
12 Mülter, M. & Zentel, R. Photochemical amplification of chiral induction in polyisocyanates. *Macromolecules* **27,** 4404–4406 (1994).
13 Mülter, M. & Zentel, R. Photochemical inversion of the helical twist sense in chiral polyisocyanates. *Macromolecules* **28,** 8438–8440 (1995).

14 Mülter, M. & Zentel, R. Interplay of chiral side chains and helical main chains in polyisocyanates. *Macromolecules* **29,** 1609–1617 (1996).
15 Mayer, S., Maxein, G. & Zentel, R. Correlation between the isomerization of side groups and the helical main chain in chiral polyisocyanates. *Macromolecules* **31,** 8522–8525 (1998).
16 Fissi, A., Pieroni, O., Angelini, N. & Lenci, F. Photoresponsive polypeptides. Photochromic and conformational behavior of spiropyran-containing poly(L-glutamate)s under acid conditions. *Macromolecules* **32,** 7116–7121 (1999).
17 Angiolini, L. & Carlini, C. Optically active polymers containing side-chain photochromic moieties. Synthesis and chiroptical properties of copolymers of trans-*N*-(4-azobenzene)maleimide with (–)-menthyl vinyl ether and (+)(S)-2-methylbutyl vinyl ether. *J. Polym. Sci. A Polym. Chem.* **29,** 1455–1463 (1991).
18 Angiolini, L., Caretti, D., Carlini, C., Altomare, A. & Solaro, R. Optically active polymers containing side-chain azobenzene moieties: photochromic and photoresponsive behavior of copolymers of *N*-(4-azobenzene)maleimide with (–)-menthyl vinyl ether and (+)-(S)-2-methylbutyl vinyl ether. *J. Polym. Sci. A Polym. Chem.* **32,** 2849–2857 (1994).
19 Reddy, P. Y., Kondo, S., Toru, T. & Ueno, Y. Lewis acid-hexamethyldisilazane-promoted efficient synthesis of *N*-alkyl- and *N*-arylimide derivatives. *J. Org. Chem.* **62,** 2652–2654 (1997).
20 Reddy, P. Y., Kondo, S., Fujita, S. & Toru, T. Efficient synthesis of fluorophore-linked maleimide derivatives. *Synthesis* **1998,** 999–1002 (1998).
21 Abiko, A. & Masamune, S. An improved, convenient procedure for reduction of amino acids to amino alcohols: use of sodium borohydride—sulfuric acid. *Tetrahedron Lett.* **33,** 5517–5518 (1992).
22 Denmark, S. E., Nakajima, N., Nicaise, O. J.- C., Faucher, A.- M. & Edwards, J. P Preparation of chiral bisoxazolines: observations on the effect of substituents. *J. Org. Chem.* **60,** 4884–4892 (1995).
23 Isobe, Y., Onimura, K., Tsutsumi, H. & Oishi, T. Asymmetric polymerization of *N*-1-naphthylmaleimide with chiral anionic initiator: preparation of highly optically active poly(*N*-1-naphthylmaleimide). *Macromolecules* **34,** 7617–7623 (2001).
24 Isobe, Y., Onimura, K., Tsutsumi, H. & Oishi, T. Asymmetric polymerization of *N*-1-anthrylmaleimide with diethylzinc-chiral ligand complexes and optical resolution using the polymer. *Polym. J.* **34,** 18–24 (2002).